Metallophysics and Advanced Technologies
Металофіз. новітні технол.
Metallofiz. Noveishie Tekhnol.
2023, vol. 45, No. 10, pp. 1179–1187
https://doi.org/10.15407/mfint.45.10.1179
Reprints available directly from the publisher

PACS numbers: 43.35.Zc, 62.20.D-, 62.20.fg, 62.30.+d, 62.65.+k, 81.40.Jj, 81.70.Cv

Characterization of a Shape-Memory Alloy Using Acoustic Techniques and Modelling of the Acoustic Signature $V(z)$

C. Larbaoui, R. Benlachemi, A. Boudour, and Y. Boumaiza

Materials Development and Analysis Laboratory, Department of Physics,
Faculty of Science, Badji Mokhtar University,
B.P. 12, Sidi Amar,
CP 23000 Annaba, Algeria

This work focuses on the characterization of CuZnAl shape-memory alloy in its 3 states (austenitic, mixed, and martensitic) by a non-destructive technique to determine its elastic properties. This technique is based on the principle of acoustic microultrasound. It allows measuring the propagation velocities of the longitudinal, transverse, and Rayleigh acoustic waves, from which the elastic constants of the material (Young's modulus E, shear modulus G) are calculated. Thus, the obtained results of the measurements allow the modelling of the acoustic signature $V(z)$ and the reflection coefficient $R(\theta)$ to compare the resulting Rayleigh velocities, which were modelled and measured experimentally in the different phases.

Key words: shape-memory alloy (CuZnAl), velocity (longitudinal, transverse, and Rayleigh), Young's modulus, shear modulus, acoustic signature $V(z)$, reflection coefficient.

Роботу присвячено характеризації стопу з пам'яттю форми CuZnAl у 3 станах (аустенітному, змішаному та мартенситному) за допомогою неруйнівної методики для визначення його пружніх властивостей. Цю методику засновано на використанні мікроультразвуку. Вона уможливлює вимірювати швидкості поширення поздовжніх, поперечних і Релейових акустичних хвиль, з яких розраховуються пружні константи матеріялу (модуль Юнґа E, модуль зсуву G). Таким чином, одержані результати мірянь уможливлюють змоделювати акустичну сиґнатуру $V(z)$ і коефіцієнт

Corresponding author: Chaima Larbaoui
E-mail: boumaizayoucef@gmail.com

Citation: C. Larbaoui, R. Benlachemi, A. Boudour, and Y. Boumaiza, Characterization of a Shape-Memory Alloy Using Acoustic Techniques and Modelling of the Acoustic Signature $V(z)$, *Metallofiz. Noveishie Tekhnol.*, **45**, No. 10: 1179–1187 (2023). DOI: 10.15407/mfint.45.10.1179

відбиття $R(\theta)$, щоб порівняти одержані Релейові швидкості, яких було змодельовано та виміряно експериментально для різних фаз.

Ключові слова: стоп з пам'яттю форми (CuZnAl), швидкість (поздовжня, поперечна та Релейова), модуль Юнґа, модуль зсуву, акустична сиґнатура $V(z)$, коефіцієнт відбиття.

(Received 14 June, 2023; in final version, 25 August, 2023)

1. INTRODUCTION

Developments in non-destructive testing (NDT) techniques have greatly contributed to the progress of new materials manufacturing methods. In this study, the acoustic microultrasound technique is used to characterize a so-called shape-memory material. There are several alloy families, the best-known ones are copper-based [1, 4], iron-based [2] and Ti–Ni-based [3]. This study is established on the latter. Shape-memory alloys (SMA) are materials widely used in many industrial applications due to their particular thermodynamic properties, namely: shape-memory effect and pseudo-elasticity (superelastic effect), *etc*.

In order to demonstrate the effects of treatments on the elastic properties of this alloy, a non-destructive technique (acoustic microultrasound) is used to measure the propagation velocities of the longitudinal, transverse, and Rayleigh waves. This allows determining the elastic properties, the acoustic signature $V(z)$ and the reflection coefficient $R(\theta)$. To verify the effects of these treatments, DSC measurement and microscopic observation are carried out to determine the transformation points and the coexistent phases in this sample.

In this study, we attempt to show the influence of the treatments that the material undergoes according to the elastic parameters and to make a comparative study between the experimental and modelled Rayleigh velocities.

2. MATERIALS AND EXPERIMENTAL TECHNIQUES

The principle of the ultrasound consists of a transducer that emits an ultrasonic wave into a fluid [5] using the following device (see Fig. 1).

Part of the wave will penetrate the material, and the other part will be reflected by the surface; then, it will be received by the transducer. The latter thus serves as both transmitter and receiver. The first echo received by the transducer is called interface echo (see Fig. 2).

Thus, the received echo corresponds to a round trip of the sound wave in the material. This allows determining the longitudinal and transverse velocities according to the travel time 'Δt' of the wave and the thickness e of the material. These parameters are related by the following equations:

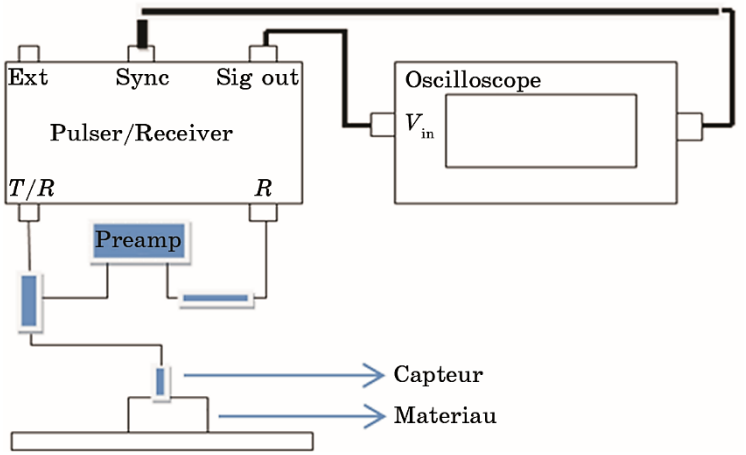

Fig. 1. Block diagram of the ultrasound scanner in reflection mode.

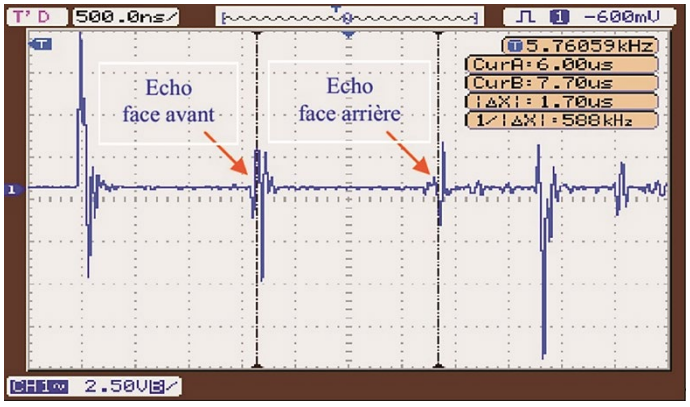

Fig. 2. Principle of microultrasound.

longitudinal velocity [6] is given by the following relation:

$$V_{\mathrm{L}} = \frac{2e}{\Delta t}; \tag{1}$$

transverse velocity is measured similarly using the displacement sensor [7], which allows showing the signal attributed to the transverse waves.

We notice that the longitudinal velocity is higher than the transverse velocity:

$$V_{\mathrm{T}} \leq \frac{V_{\mathrm{L}}}{\sqrt{2}}. \tag{2}$$

The resulting measurements of these velocities allow calculating the elastic parameters (Young's modulus E, shear modulus G) [6]:

$$E = \rho V_{\mathrm{L}}^2, \tag{3}$$

$$G = \frac{E}{2(1+\upsilon)}. \tag{4}$$

It is clear that, for any material considered and whatever it is belonging, Young's modulus E is higher than shear modulus G.

Rayleigh wave velocity is an intrinsic parameter of the material. It can be calculated according to the law of Viktorov [8, 9]:

$$V_{\mathrm{R}} = V_{\mathrm{T}} \frac{0.718 - (V_{\mathrm{T}} / V_{\mathrm{L}})^2}{0.750 - (V_{\mathrm{T}} / V_{\mathrm{L}})^2}. \tag{5}$$

The use of the reflection coefficient $R(\theta)$ and the acoustic signature $V(z)$ also give the value of Rayleigh velocity.

The expression $R(\theta)$ is calculated by using the mechanical balance and the continuity of stress and displacement at the surface. It was developed by Brekhovskikh [6, 8].

The reflection coefficient for massive materials is given by the following expression [9]:

$$R(\theta) = \frac{\dfrac{V\rho_{\mathrm{sol}}}{\cos\theta}\cos^2(2\theta)\dfrac{2\rho_{\mathrm{sol}}V_{\mathrm{T}}}{\cos\theta_{\mathrm{L}}}\sin^2(2\theta) - \dfrac{\rho_{\mathrm{liq}}V_{\mathrm{liq}}}{\cos\theta}}{\dfrac{V\rho_{\mathrm{sol}}}{\cos\theta}\cos^2(2\theta)\dfrac{2\rho_{\mathrm{sol}}V_{\mathrm{T}}}{\cos\theta_{\mathrm{L}}}\sin^2(2\theta) + \dfrac{\rho_{\mathrm{liq}}V_{\mathrm{liq}}}{\cos\theta}}. \tag{6}$$

The acoustic signature $V(z)$, which is necessary for the microcharacterization of a material, is determined from the reflection coefficient. It is obtained from defocusing (distance z between the focal plane and the interface (solid–liquid). Its expression is given by the following relation [10]:

$$V(z) = \int_0^{\theta_{\max}} P^2(\theta) R(\theta) e^{2jk_0 \cos\theta} \sin\theta\cos\theta d\theta, \tag{7}$$

where $j = (-1)^{1/2}$, $\theta_{\max}$ is opening of the lens, $P^2(\theta)$ is pupil function, K_0 is wave vector in liquid. From this relation, we can determine the different propagation velocities of the waves according to the different treatments of the acoustic signature $V(z)$. In this case, the Fourier Transform (FT) is used to access these different speeds:

$$V_{\mathrm{R}} = \frac{V_{\mathrm{liq}}}{[1 - (1 - V_{\mathrm{liq}} / (2f\Delta z))]^{1/2}}. \tag{8}$$

3. RESULTS AND DISCUSSIONS

A CuZnAl sample is used. The sample condition is defined by the use of DSC and the optical microscope. It undergoes homogenization treatments at 850°C for 15 minutes (Table 1).

The sample is immersed in the experimental ultrasound device with a coupling medium (water) at $T < M_F$, and it is left to heat gradually to $T > A_F$.

Then, the influence of these thermic treatments (with their different states) is studied on the longitudinal velocity.

For the three sample states (austenitic, mixed, and martensitic ones), several measurements are made at different points on the shape-memory sample. The results obtained are provided in Table 2.

We note for these three states that the propagation velocities of the waves are different that implies that the elastic properties differ from one state to another.

Another study is conducted by using the micro-ultrasound technique to determine the different points (M_F, M_S, A_S, A_F) from the experimental velocities according to ($V_L = f(T)$) heating (see Fig. 3). This confirms the DSC results for different points.

3.1. Acoustic Observation of the Austenitic and Martensitic Structures

The structures of the CuZnAl samples are studied with an optical microscope to display the different metallurgical phases and their spatial distribution on the surface of this alloy.

The samples are prepared for microstructural analysis by polishing the surface using sandpaper followed by felt paper and alumina paste to obtain a highly polished surface. Then, the samples are etched using the $FeC_{13}{\cdot}3H_2O$ etching solution. The microstructural analysis of the

TABLE 1. Transformation points of the CuZnAl sample.

CuZnAl sample	M_S	M_F	A_S	A_F
	2	–5	4	12

TABLE 2. Elastic parameters of the CuZnAl sample.

Studied CuZnAl alloy	V_L, m/s	V_T, m/s	ρ	E, GPa	G, GPa
Austenitic state (A)	5240.96	2830.12	7400	203.26	78.78
Mixed state (A + M)	4390.7	2370.98	7400	142.65	55.29
Martensitic state (M)	3722.66	2010.24	7400	102.55	39.74

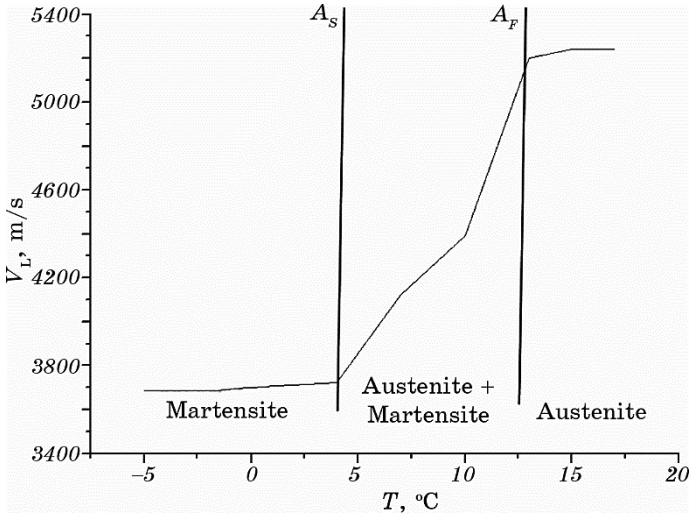

Fig. 3. Longitudinal velocity as function of temperature.

samples is carried out with the help of the AXIO Imager.A2m optical microscope.

Figure 4 shows the austenite micrograph at room temperature and the martensite micrograph.

Figures 4, *a* and *b* show the austenitic microstructure as cast and the formation of the martensite variants during the quenching. We can observe that a complete transformation from austenite to martensite occurs in Fig. 4, *c*.

Table 2 shows the values of the measured velocities of the three states studied. It can be noticed that in the case of the martensitic state, the velocity is inferior to that of the austenitic state. This is in good agreement with the bibliographical references.

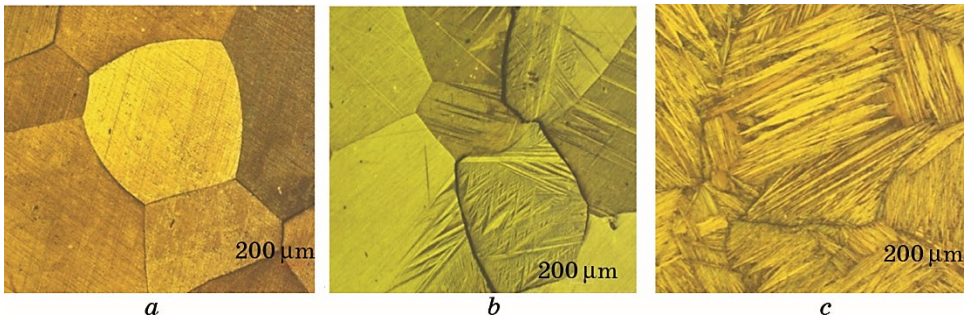

Fig. 4. Austenitic structure (*a*), mixed structure (A + M) (*b*), martensitic (*c*).

3.2. Study of Phase and Amplitude Variations According to the Austenitic, Mixed and Martensitic States

This part is dedicated to the modelling of the reflection coefficient $R(\theta)$ and the acoustic signature $V(z)$ based on the experimental results obtained from the longitudinal and transverse velocities according to the different states (austenitic–mixed–martensitic). Figure 5 shows the change in the phase and the amplitude of the reflection coefficient $R(\theta)$ of the Cu–Zn–Al samples at a frequency $f = 50$ MHz. We can quantify the effect of the states on the CuZnAl shape-memory alloy sample. In the martensitic state (phase 3), the sample is at a temperature of –5°C ($T < M_F$) for 15 seconds. Then, it is heated at $M_S < T < A_S$ (phase 2 (mixed)). For the final state, the temperature is raised to $T > A_S$ (phase 1 (austenitic)).

3.3. Study of the Acoustic Signature $V(z)$

We note that all acoustic signatures $V(z)$ obtained are pseudo-periodic regardless of the state of the sample. However, the pseudo-period 'Δz' vary from one state to another, thus giving different Rayleigh velocity results.

We also note from these curves that the difference of the sample states affects the variation of the phase, the amplitude and the acoustic signature $V(z)$.

3.4. Rayleigh Velocity Obtained from the Reflection Coefficient $R(\theta)$

This part is dedicated to the modelling of the reflection $R(\theta)$ and the

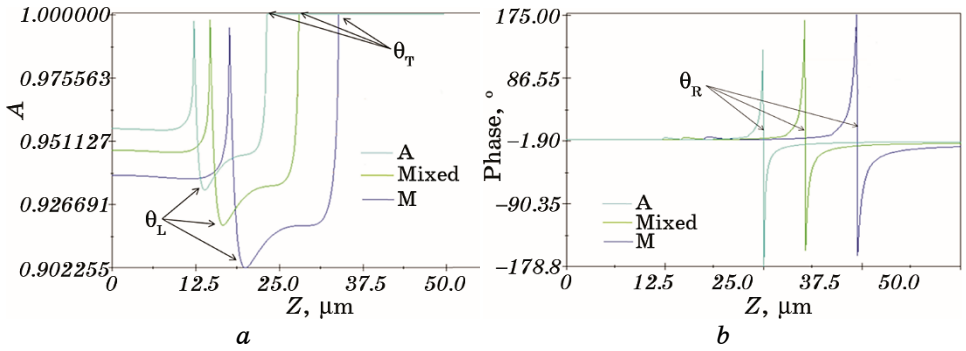

Fig. 5. Phase variations of the CuZnAl alloy at different thermic states (*a*), amplitude variations of the reflection coefficient $R(\theta)$ of the CuZnAl alloy at different thermic states (*b*).

TABLE 3. Rayleigh velocity of CuZnAl sample.

Studied CuZnAl alloy	Critical angle, °	Rayleigh velocity, m/s	
		Viktorov (experimental)	Snell–Descartes (theoretical)
Austenitic state (A)	25	2633.24	2609.29
Mixed state (A + M)	30.11	2206.04	2198.69
Martensitic state (M)	36.93	1870.79	1835.76

acoustic signature $V(z)$ from the experimental results obtained. Table 3 recapitulates the Rayleigh velocity results obtained using two different approaches.

Figure 6 shows the acoustic signature $V(z)$ of three states (martensitic, mixed, and austenitic states) of the Cu–Zn–Al sample at a frequency $f = 50$ MHz.

4. CONCLUSION

Velocities of the acoustic waves (longitudinal, transverse and Rayleigh ones) are determined experimentally at different states of the CuZnAl shape-memory alloy. Table 2, where the results are listed, shows that the velocities and the elastic parameters are different in the three states. Surface wave propagation velocities (Rayleigh) are determined accord-

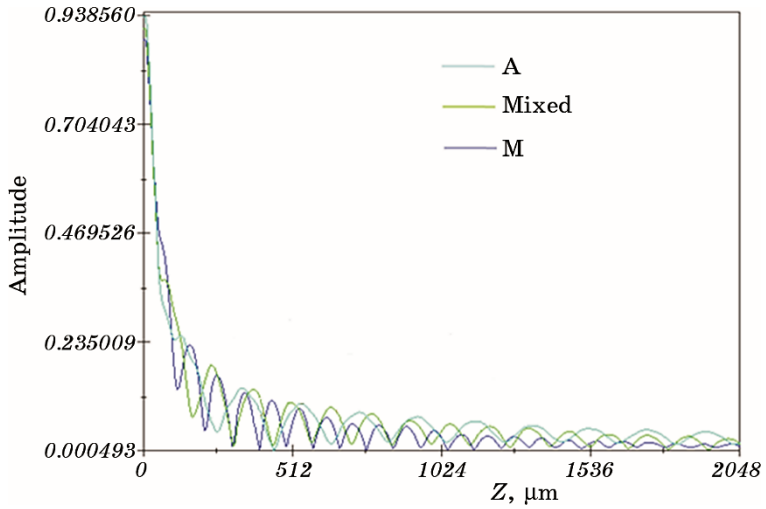

Fig. 6. Acoustic signature $V(z)$ of the CuZnAl sample at different states (austenitic, mixed, and martensitic), $f = 50$ MHz, $e = 1$ mm.

ing to Viktorov approximate formula (experimentally) and the phase change (function of reflection) for different states. We notice that the values of the velocities are very close yet different from one state to another. This study attempts to show the influence of the structural states on the elastic parameters of the sample at different phases.

REFERENCES

1. M. T. Cao-Rial, C. Moreno, and P. Quintela, *Applied Mathematical Modelling* **77**, Pt. 1: 439 (2020).
2. K. K. Alaneme and E. A Okotete, *Eng. Sci. Technol.*, **19**, Iss. 3: 1582 (2016).
3. S. Chouf, M. Morin, S. Belkahla, and G. Guénin, *Mater. Sci. Eng. A*, **438–440**: 671 (2006).
4. M. Benchiheub, S. Belkahla, and G. Guénin, *La Revue de Métallurgie*, 1471 (2000).
5. R. Dasgupta, A. K. Jain, P. Kumar, S. Hussein, and A. Pandey, *Mater. Res. Technol.*, **3**, Iss. 3: 264 (2014).
6. Z. Wang and A. M. Korsunsky, *Encyclopedia of Smart Materials* (Elsevier: 2022), p. 239.
7. J. David and N. Cheeke, *Fundamentals and Applications of Ultrasonic Waves* (Boka Raton: CRC Press: 2002).
8. L. M. Brekhovskikh and O. A. Godin, *Acoustic of Layered Media I: Plane and Quasi-Plane Waves* (Berlin: Springer-Verlag: 1990).
9. I. A. Viktorov, *Rayleigh and Lamb Waves. Physical Theory and Application* (New York: Springer: 1967).
10. T. Tahraoui, Y. Boumaiza, and A. Boudour, *Optoelectronics and Advanced Materials*, **4**, No. 11: 1771 (2010).
11. A. Benbelghit, D. Boutassouna, B. Helifa, and I. K. Lefkaier, *NDT E International*, **39**: 76 (2006).